Microtubule-dependent protein trafficking promotes apical constriction during tissue invagination

Thao Phuong Le[1], SeYeon Chung[1, *]

1 Department of Biological Sciences, Louisiana State University, Baton Rouge, LA 70803, USA

*Author for correspondence: seyeonchung@lsu.edu

Abstract

The formation of an epithelial tube is a fundamental process for organogenesis. Mechanisms underlying coordination between actomyosin and microtubules (MTs) during tube formation is beginning to be elucidated. During the *Drosophila* embryonic salivary gland (SG) invagination, Folded gastrulation (Fog)-dependent Rho-associated kinase (Rok) promotes contractile apical myosin formation to drive apical constriction. MTs are also crucial for the effective change in apical area and are required for forming and maintaining apicomedial myosin. Here, we show that MT-dependent intracellular trafficking has a role in regulating apical constriction during SG invagination. Key components involved in protein trafficking, including dynein heavy chain, Rab11 and Nuclear fallout (Nuf), are apically enriched near the invagination pit in a MT-dependent manner during SG invagination. This enrichment is crucial for apical constriction as disruption of the MT networks or intracellular trafficking impairs formation of apicomedial myosin, which leads to apical constriction defects. We show that apical transport of several proteins along MTs, either in a Rab11-dependent or independent manner, mediates clustered apical constriction during SG invagination. Key proteins that are transported include the Fog ligand, the apical determinant protein Crb, a key adherens junction protein E-Cad and the scaffolding protein Bazooka/Par3, and knockdown of these genes in the SG results in apical constriction defects. These results define a role of MT-dependent intracellular trafficking in regulating the actomyosin networks as well as cell junctions to coordinated cell behaviors during tubular organ formation.

Introduction

The formation of three-dimensional tubes by invagination from flat epithelial sheets is a fundamental process in forming organs such as lungs and kidneys (Andrew and Ewald, 2010). To enter the third dimension, cells must change their shapes and positions relative to each other. A major cellular process that is observed during epithelial tube formation is apical constriction, a universal cell shape change that is linked to tissue bending, folding and invagination (Martin and Goldstein, 2014; Sawyer et al., 2010). During apical constriction, the apical side of the epithelial cells constricts, causing a columnar or cuboidal cell to become wedge-shaped (Martin and Goldstein, 2014; Sawyer et al., 2010). Manipulation of apical constriction in a group of cells impacts both local and global tissue shape directly, suggesting a critical role of apical constriction in forming proper tissue architecture (Guglielmi et al., 2015; Chung et al., 2017; Izquierdo et al., 2018).

A common machinery that drives apical constriction includes actin filament (F-actin) networks and the molecular motor non-muscle myosin II (hereafter referred to as myosin). The actomyosin cytoskeletal complex generates contractile forces that are exerted on adherens junctions that are attached to actin cytoskeleton to shrink the apical domain of cells (Martin and Goldstein, 2014). Studies in the past decade revealed important functions of different actomyosin structures in epithelial tissue morphogenesis. Particularly, several studies in *Drosophila* revealed a distinct population of apical medial actomyosin that shows a pulsatile behavior that generates a pulling force to drive apical constriction in different tissues (hereafter referred to as apicomedial myosin; Martin et al., 2009; Rauzi et al., 2010; Booth et al., 2014; Chung et al., 2017). In early *Drosophila* embryos, apicomedial myosin is created in response to signaling by the Folded gastrulation (Fog) ligand and its G protein-coupled receptors (GPCRs) (Manning et al., 2013; Kerridge et al., 2016), and is regulated by apical Rho-associated kinase (Rok) (Mason et al., 2013).

Using the *Drosophila* embryonic salivary gland (SG) as a model, we previously showed that apical constriction is regulated in a highly coordinated and spatiotemporally-controlled manner during epithelial tube formation (Chung et al., 2017). The *Drosophila* embryo forms two SG tubes from two epithelial placodes on the ventral surface, through invagination of SG cells from the dorsal posterior region of each placode (Chung et al., 2014). We showed that during invagination, SG cells undergo apical constriction in a spatially biased way. In the SG, a small group of cells in the

dorsal/posterior region of the placode begins to constrict first. As those cells internalize to form the invagination pit, more cells anterior to the pit undergo clustered apical constriction in a Fog signaling-dependent manner to internalize sequentially (Chung et al., 2017; Fig. 1A). In the absence of *fog*, SG cells fail to accumulate Rok and apicomedial myosin in the apicomedial region of the cells, and constricting cells are no longer clustered near the invagination pit, but dispersed (Chung et al., 2017).

Emerging evidence suggests an important role of another key cytoskeletal component, the microtubule (MT) network, in tissue invagination (Booth et al., 2014; Ko et al., 2019). In early *Drosophila* embryos, MTs were shown to stabilize actomyosin intercellular attachments in epithelia during mesoderm invagination (Ko et al., 2019). In the *Drosophila* SG, MTs also play a crucial part in forming and maintaining the apicomedial myosin network during invagination, suggesting an interplay between two cytoskeletal networks (Booth et al., 2014). Particularly, in the *Drosophila* SG, the MT cytoskeleton near the invagination pit undergoes a 90o change in alignment relative to the apicobasal axis, leading to a network of longitudinal MT bundles (Booth et al., 2014). The minus ends of MTs face the apical domain of the cells and interact with the apicomedial myosin in the SG, and disruption of MTs causes loss of apicomedial myosin and loss of apical constriction during SG invagination (Booth et al., 2014).

A major role of MTs is to serve as tracks in intracellular transport, raising a possible role of MTs in turnover of membrane receptors and adhesion molecules through endo- and exocytosis to regulate apical constriction. Several lines of evidence suggest an important role of the endocytic pathway in apical constriction in both in vitro and in vivo systems. A study using Madin Darby Canine Kidney cells showed that Dynamin 2, a key component of clathrin-dependent endocytosis and the only dynamin in epithelial cells, orchestrates the actomyosin cytoskeleton for epithelial maintenance and apical constriction (Chua et al., 2009). Also, during *Xenopus* gastrulation, disrupting endocytosis with dominant-negative dynamin or Rab5, a key regulatory factor for early endocytic events, perturbs apical constriction and invagination of cell sheets (Lee and Harland, 2010). Moreover, in the developing neural tube in *Xenopus*, asymmetric enrichment of the recycling endosome marker Rab11 at the medial apical junctions is critical for apical constriction, suggesting that anisotropic membrane trafficking has a key role in apical constriction (Ossipova et al., 2014). However, cargo proteins that are transported to regulate apical constriction are not well known.

We demonstrate that key endocytic markers, including Rab11 and its binding partner Nuclear fallout (Nuf), are enriched in the apical domain of the SG cells during invagination in a MT-dependent manner. We further show that disruption of intracellular trafficking leads to decrease of accumulation of apicomedial Rok and myosin and causes uncoordinated apical constriction in the SG. Our data suggest that apical transport of several proteins, including the Fog ligand, the apical determinant protein Crumbs (Crb), as well as E-Cadherin (E-Cad) and the scaffolding protein Bazooka/Par3 (Baz/Par3), is compromised when the MT networks are disrupted, which affects apical constriction during SG invagination.

Results

Intracellular trafficking components are apically enriched near the invagination pit

To test a role of the intracellular trafficking machinery in spatially biased signaling activation and protein accumulation during SG invagination, we analyzed subcellular localization of proteins that are involved in vesicle trafficking in the SG. Several endosomal markers were highly enriched in the apical domain of the SG cells near the invagination pit, including Rab11, a recycling endosome marker, Nuclear fallout (Nuf), a putative binding partner for Rab11, and Sec15, an exocyst complex component and effector for Rab11, suggesting active trafficking activities in the region where cells are apically constricting (Figs. 1C-D'; data not shown). Using labeling with E-Cadherin (E-Cad), an adherens junction marker, and CrebA, a SG nuclear marker, we segmented apical cell outlines. (Figs. 1B, B'). Average intensity of Rab11 or Nuf in the apical domain of each cell showed a negative correlation with the apical area of cells in the entire SG (Fig. 1E).

Rab5, an early endosome marker, was also upregulated near the pit, suggesting active endocytosis in this region (Fig. S1). Rab7, a late endosome marker, however, did not show any enrichment but localized as big punctate structures in the cytoplasm of the SG cells in the entire placode, suggesting that not all endocytic markers are upregulated near the pit during SG invagination (Fig. S1). Dynein heavy chain, a subunit of the dynein motor complex that transports cargos along the MTs toward their minus ends, also showed upregulation near the invagination pit (Figs. 1F-G'). Overall, our results suggest active protein trafficking, possibly both endo- and exocytosis, in the dorsal/posterior region near the invagination pit during SG invagination. The negative correlation

between apical area and intensity of several components of intracellular protein trafficking also suggests a role of intracellular trafficking in apical constriction during SG invagination.

Disruption of MTs results in uncoordinated apical constriction, reduction of apical vesicle numbers, and mislocalization of Rab11/Nuf to the cytoplasmic and basolateral region

Like many epithelial cells, MT minus- and plus-ends face the apical and the basal domain of the SG cells, respectively (Myat and Andrew, 2002; Booth et al., 2014). Strong apical enrichment of Rab11 and Nuf in the SG cells near the invagination pit led us to test if these vesicle markers are associated with vertically aligned MTs. Indeed, co-immunostaining of acetylated α-tubulin and Rab11 showed a partial overlap of the two proteins at the apical region of the SG cells (Figs. 2A'-A''').

To test if Rab11 enrichment in the apical region of the SG cells is dependent on the MT networks, we disrupted MTs by overexpressing Spastin, a MT-severing protein (Sherwood et al., 2004), in the SG using the SG-specific fkh-Gal4 driver. In wild type SGs, acetylated α-tubulin was observed abundantly in the apical domain of cells in the whole placode. When Spastin was overexpressed, acetylated α-tubulin signals were strongly reduced, revealing loss of stable MT filaments in the SG (Figs. 2B-C'''). Importantly, quantification of the intensity of Rab11 and Nuf showed that, compared to control SGs (Figs. 1C-D'), SGs with disrupted MTs showed strong reduction of both proteins in the apical domain of the SG cells near the invagination pit (Figs. 2E-G). This data suggests that the MT networks are required for apical enrichment of Rab11 and Nuf during SG invagination.

Analysis of Spastin-overexpressing SGs at stage 16 revealed that disruption of MTs resulted in short SG tubes with a thin lumen compared to control SGs of the same stage (Figs. 2H and I). Strikingly, whereas the majority of Rab11- and Nuf-positive vesicles localized in the apical region of the cells in control SGs, disruption of MTs led to mislocalization of Rab11- and Nuf-positive vesicles to the cytoplasmic and basolateral regions of the SG cells. (Figs. 2I-I'''). Mislocalized Rab11 and Nuf overlapped, suggesting that they work together as a complex. Our data suggest that MTs are required for apical trafficking of Rab11/Nuf vesicles during SG tubes formation.

Rab11 and the dynein motors are required for apical constriction in the SG

Overexpression of Spastin caused defective apical constriction during SG invagination (Booth et al., 2014; Figs. 2D and D'). To test a possibility that compromised apical constriction caused by disruption of MTs is linked to the reduction of Rab11/Nuf vesicular transport, we disrupted the function of Rab11 by overexpressing a dominant-negative form of Rab11 (Rab11S25N-YFP; hereafter referred to as Rab11-DN) in the SG. Quantification of percentage and cumulative percentage of cells of different apical area revealed that, compared to control, SGs overexpressing Rab11-DN showed more cells with bigger apical area, suggesting a role of Rab11 in apical constriction during SG invagination (Figs. 3A, B).

As Dynein heavy chain was also enriched near the invagination pit (Fig. 1F-G'), we hypothesized that dynein motors might have a role in trafficking key proteins along MTs to control apical constriction during SG invagination. Indeed, zygotic knockdown of *dynein heavy chain 64C* (*Dhc64C*) in the SG showed more cells with bigger apical areas at the time of internalization, suggesting defective apical constriction (Figs. 3C, C'). The relatively mild apical constriction defects could be due to strong maternal contribution as dynein is essential for oogenesis and has a critical role in early embryo development (Li et al., 1994). To knock down both maternal and zygotic pools of *Dhc64C*, we used a maternal driver matα-Gal4, along with the SG-specific fkh-Gal4. Embryos knocked down both maternal and zygotic pools of *Dhc64C* developed until late stages of embryogenesis but showed a range of morphological defects, some of which are quite severely disrupted (data not shown). SG cells in the embryos with relatively mild morphological defects still invaginated and formed a tube, but 3D-rendering revealed that most SGs formed an enlarged invagination pit and showed bigger apical area in individual cells compared to control SGs (Fig. 3F).

Klarsicht (Klar), the *Drosophila* Klarsicht-Anc-Syne Homology (KASH) domain protein that indirectly interacts with the MT cytoskeleton through the MT motor cytoplasmic dynein (Gross et al., 2000), has been reported in mediating apical transport in the SG (Myat and Andrew, 2002). We therefore tested for a role of *klar* in apical constriction during SG invagination. SGs of *klar* mutant embryos also showed mild apical constriction defects (Figs. 3D, D'). Quantification of percentage and cumulative percentage of cells (Figs. 3E, F) of different apical area showed a small,

but significant increase in the number of cells with bigger apical area compared to control SGs. Overall, our data suggest a role of the intracellular trafficking machinery in regulating apical constriction during SG invagination.

Compromised intracellular trafficking leads to failure in accumulation of apicomedial Rok and reduction of apicomedial myosin formation in the SG cells

We previously showed that Fog signaling-dependent accumulation of apical medial Rok is required for apicomedial myosin formation for coordinated apical constriction in SG cells (Chung et al., 2017). Therefore, using a ubiquitously expressed GFP-tagged Rok transgene (Rok-GFP; Abreu-Blanco et al., 2014). we tested Rok signals in the embryos where MT-dependent vesicular transport was reduced. In control SGs, Rok accumulated at the apicomedial region of the constricting cells to form big punctate structures near the invagination pit (Figs. 4A-A''). On the other hand, in MT-disrupted SGs, apical Rok signals were reduced and Rok was not accumulated in apical region of constricting cells (Figs. 4B-B''). Our results support the previous finding that Spastin overexpression inhibits formation of apicomedial myosin during SG invagination (Booth et al., 2014). We also tested accumulation of apicomedial Rok-GFP signals in *Dhc64C* RNAi SGs. Reduction of *Dhc64C* levels caused dispersed Rok signals on the apical surface of constricting cells near the pit (Fig. 4C-C''). Similarly, Rok-GFP was accumulated less profoundly in the apicomedial region of SG cells in *klar* mutants, although some big punctate structures were still observed (Figs. 4D-D'').

We next tested apicomedial myosin formation in SG cells when intracellular trafficking pathway was compromised. In control, sqh-GFP (a functional GFP-tagged version of the myosin regulatory light chain; Royou et al., 2004), showed a strong apicomedial myosin web in the constricting cells near the invagination pit (Figs. 4E-E''). In *Dhc64c* RNAi SGs, apicomedial myosin was decreased near the invagination pit (Figs. 4F-F''). Our quantification showed that cells with and without a strong apicomedial myosin web had smaller and bigger apical areas, respectively, suggesting that defective apical constriction in *Dhc64* RNAi could be due to failure in apicomedial myosin formation (Fig. 4H). Similar reduction of apicomedial myosin was observed in *klar* mutant SGs

(Figs. 4G-G''). Our data suggest that vesicular trafficking regulates apical accumulation of Rok and apicomedial myosin formation during SG invagination.

Fog signaling activity is reduced when MTs are disrupted

Since Rok accumulation, apicomedial myosin formation, and subsequent coordinated apical constriction are Fog-dependent (Chung et al., 2017), we tested if apical constriction defects caused by disruption of protein trafficking were due to disrupted Fog signaling. Although the existing Fog antibody detected the endogenous Fog protein in the SG lumen at later stages, the signals at stage 11 were not strong enough to show precise subcellular localization of Fog in the SG. We therefore overexpressed Fog in the SGs to saturate the transport system and test a role of MTs in transporting Fog in this sensitized background. Interestingly, we observed dramatic changes of the SG cell morphology when Fog was overexpressed. In the control SG, cells mostly maintained straight adherens junctions (Figs. 5A' and D). In Fog-overexpressing SGs, however, cell junctions were highly convoluted (Figs. 5B' and D'). Moreover, Fog-overexpressing SG cells over-accumulated Rok-GFP in the apicomedial region (Fig. 5B'''). Over-accumulation of Rok by Fog overexpression was consistent with our previous data that Fog mediates apicomedial Rok accumulation (Chung et al., 2017). When we co-overexpressed Fog and Spastin, the wiggly junctional phenotypes were partially suppressed (Figs. 5C' and D''). Moreover, over-accumulation of Rok-GFP caused by Fog overexpression was also suppressed when Fog and Spastin were co-overexpressed, suggesting that disruption of MTs suppressed overactivated Fog signaling (Fig. 5C''). Our data suggest that MTs regulate Fog signaling activity, possibly by regulating transport of the Fog ligand during SG invagination.

MT-dependent intracellular trafficking regulates apical transport of Crb in the SG

Transport of several key apical and junctional proteins is dependent on MTs and Rab11 (Khanal et al., 2016, Le Droguen et al., 2015, Jouette et al., 2019). One such protein is an apical transmembrane protein Crb. In the *Drosophila* ectoderm, Rab11 helps maintain apical Crb (Roeth et al., 2009). In *Drosophila* follicle cells, Crb is apically transported along MTs by the dynein motor (Aguilar-Aragon, et al., 2019). Moreover, in the *Drosophila* trachea, loss of *crb* impairs

apical constriction during the internalization process (Letizia et al., 2011). Since Crb is upregulated near the invagination pit during SG invagination (Fig. 6A), we asked if MT-dependent apical transport of Crb is required for coordinated apical constriction in the SG.

We did not detect significant changes in localization or intensity of the endogenous Crb protein in MT-disrupted SGs (data not shown). Therefore, using the same strategy as we used for testing a role of MTs in Fog trafficking (Figs. 5B-B'''), we overexpressed Crb in the SG to test if disruption of MTs affects apical transport of Crb. A similar approach was taken in a recent study, where they showed that overexpression of Crb provided a highly sensitive genetic background for identifying components involved in Crb trafficking (Aguilar-Aragon et al., 2019). Consistent with previous findings that Crb expression expands apical membranes in epithelial cells (Wodarz et al. 1993; Chung and Andrew, 2014), overexpression of Crb resulted in increased apical area of SG cells compared to control (Figs. 6A-B'). When we co-overexpressed Crb and Spastin, the increased apical area phenotype was suppressed (Figs. 6C-C''), and Crb was mislocalized to big cytoplasmic punctate structures near the basolateral domain. Mislocalized Crb largely overlapped with Rab11-positive vesicles both at stage 11 (Figs. 6D-D''') and stage 16 (Figs. 6E-F'''), suggesting that apical transport of Crb in the SG is dependent on Rab11 and MTs.

To test a role of Crb in regulating apical constriction during SG invagination, we knocked down c*rb* in SGs. Reduction of c*rb* resulted in increase of cells that have bigger apical area compared to control (Figs. 7A-B', E). This data, along with apical transport of Crb by Rab11 and MTs (Figs. 6D-D'''), suggest that proper Crb levels in the apical domain is important in apical constriction during SG invagination. In summary, our results suggest a role of Rab11 in apical transport of Crb along MTs in the SG and a role of Crb in regulating apical constriction during SG invagination.

Key apical and junctional proteins, including Crb, E-Cad and Bazooka/Par3, play a role in regulating apical constriction

During apical constriction, contractile forces generated by the actomyosin complex are exerted on adherens junctions that are coupled to the apical actin networks. Disrupted adherens junctional components resulted in actin-myosin contractions that fail to pull the apical circumference inwards efficiently (Dawes-Hoang et al., 2005; Sawyer et al., 2009; Roh-Johnson et al., 2012). Consistent

with these findings, knockdown of *E-Cad* and b*az* resulted in defective apical constriction in the SG (Fig. 7C-D'). Quantification of the percentage of cells and cumulative percentage of cells of different apical areas showed a significant reduction in the number of constricting cells in *baz* RNAi SGs (Fig. 7E). *E-Cad* RNAi SGs also showed a similar trend, although with less statistical significance (Fig. 7E). We did not detect significant changes in protein levels of E-Cad or Crb when we knocked down either gene using RNAi (Figs. 7B and C; data not shown), suggesting that subtle changes in protein levels or turnover still can affect apical constriction. At later stages, SG cells with knockdown of *crb*, *E-Cad* or *baz* still made a relatively normal tube except for a non-uniform diameter of the lumen in *E-Cad* RNAi SGs (Fig. 7G), suggesting a robustness of SG formation. In stage 16 *E-Cad* RNAi SGs, junctional E-Cad signals were discontinuous, and lateral E-Cad signals were strongly reduced compared to control (Figs. 7F-G').

To test a role of MTs in trafficking E-Cad and Baz in the SG, we used the same strategy as for Fog and Crb. Using *UAS-Shotgun-GFP (shg,* the gene encoding E-Cad) and UAS-Baz-GFP, we co-overexpressed E-Cad or Baz with Spastin in the SG. Overexpression of E-Cad-GFP alone did not result in overt morphological defects in the SG, and punctate E-Cad-GFP signals mostly overlapped with E-Cad signals at adherens junctions (Figs. 6G-G'''). Strikingly, co-overexpression of E-Cad-GFP and Spastin resulted in aggregation of E-Cad-GFP to the basolateral region of the cells (Figs. 6H-H'''), suggesting apical trafficking of overproduced E-Cad is compromised by disruption of the MT networks. Overexpression of Baz-GFP in the SGs caused enlarged lumen (Figs. 6I-I'''). Baz-GFP signals were detected mostly at adherens junction, but small punctate structures were also detected in the cytoplasm (Fig. 6I'). Co-overexpression of Spastin suppressed the enlarged lumen phenotype caused by Baz overexpression (Figs. 7J-J'''). Importantly, Baz-GFP levels were less abundant at adherens junctions and more cytoplasmic punctate structures were observed in the basolateral region (Fig. 7J''). Overall, our data suggest MT-dependent apical trafficking of several key proteins, including Crb, E-Cad and Baz, in the SG. Our results further suggest that proper levels of these proteins is important for apical constriction during SG invagination.

Reducing Crb, E-Cad and Baz/Par3 affects apical accumulation of Rok and apicomedial myosin formation

To test if apical constriction defects observed in *crb*, *E-Cad* and *baz* RNAi SGs are linked to apicomedial myosin formation, we analyzed apical Rok-GFP signals and myosin levels in SGs with *crb, E-Cad* or *baz* knockdown. Indeed, knockdown of *crb*, *E-Cad* or *baz* resulted in dispersed Rok-GFP signals in the apical region of cells near the invagination pit (Figs. 8B-D'') compared to control (Figs. 8A-A''). Myosin levels were also reduced in *crb, E-Cad* or *baz* RNAi SGs (Figs. 8F-H'', I). Both in control and the RNAi SGs, apica areas and myosin intensities displayed a negative correlation, but greater variability was observed in Crb, E-Cad and Baz-compromised SG cells (Fig. 8I). This data suggest that apical constriction defects observed in SGs reducing Crb, E-Cad or Baz are, at least in part, due to failure in accumulating apicomedial Rok that affects apicomedial myosin formation in SG cells. Taken together, our results suggest a role of apical and junctional proteins in regulating apical constriction via mediating apicomedial Rok and myosin during SG invagination.

Discussion

Despite accumulating evidence, how intracellular trafficking functions during apical constriction has not been clear. Using the *Drosophila* SG, a well-established model for epithelial tube formation, we demonstrate that MT-dependent apical transport of proteins is critical for apical constriction during tissue invagination. Several key endocytic markers such as Rab11 and Nuf are enriched at and near the invagination pit, suggesting active vesicular transport in this region during SG invagination. Enrichment of Rab11 and Nuf is dependent on the MT networks, and this enrichment is important for proper apical constriction during SG invagination as disruption of MTs or vesicular trafficking impairs apical constriction. Additionally, Dhc is also enriched near the invagination pit, and Dhc and Klar (dynein heavy chain regulator) are required for apical constriction in SGs. Our data support a model that MT-dependent apical transport of the Fog ligand, which mediates apicomedial myosin formation, as well as key apical and junctional proteins, including Crb, E-Cad and Baz, is crucial for apical constriction during SG invagination. This work converges actomyosin and MT-dependent intracellular trafficking.

Roles of MTs in apical constriction during SG invagination

MTs have been shown to have a crucial role in stabilizing apical myosin both in early *Drosophila* embryos and in the *Drosophila* SG (Booth et al., 2014; Ko et al., 2019). Particularly in the SG, MTs interact with apicomedial myosin via Short stop, the *Drosophila* spectraplakin, emphasizing a direct interplay between the MT and the apical myosin networks (Booth et al., 2014). Our data reveals another role of MTs in regulating protein trafficking to control the apical myosin networks during tissue invagination. During SG invagination, the MT cytoskeleton near the invagination site undergoes a 90o change in alignment relative to the apicobasal axis, leading to a network of longitudinal MT bundles (Booth et al., 2014). This region correlates with localized Fog signaling activity and clustered apical constriction (Chung et al., 2017). Our data shows that apical enrichment of key endocytic markers in the same area is dependent on MTs and that this enrichment is important for forming the apicomedial myosin networks (Figs. 1-4), suggesting a link between localized protein trafficking along MTs to apical myosin regulation.

A role of Rab11 and endocytosis in apical constriction has also been shown during *Xenopus* gastrulation and neural tube formation (Lee and Harland, 2010; Ossipova et al., 2014). Particularly, myosin activation is regulated by Rab11 function, suggesting a conserved role of intracellular trafficking in regulating the apical actomyosin networks in different systems. A recent study in early *Drosophila* embryos also suggested a role of membrane trafficking in apical constriction (Miao et al., 2019). During *Drosophila* gastrulation, Rab35 and the Sbf RabGEF direct the plasma membrane to Rab11 endosomes through a dynamic interaction with Rab5 endosomes (Miao et al., 2019), suggesting a convergence of actomyosin and endocytic function.

At later stages of tubular organ development, MT and dynein-mediated apical enrichment of vesicular markers functions in apical distribution of junctional proteins. During branching morphogenesis in *Drosophila* trachea, MTs and dynein motors have a critical role in proper localization of junctional proteins such as E-Cad and Baz/Par3 (Le Droguen et al., 2015). This is consistent with our observations in the late stage SGs (Fig. 6), suggesting a conserved role of MT-dependent intracellular trafficking in junctional remodeling and stabilization during epithelial tube formation. Our data suggests that proper levels of these proteins are also important for tissue invagination at the beginning of epithelial tube formation. Zygotic knockdown of *crb*, *E-Cad* or

baz barely changes the protein levels at the time of tissue invagination to the level that can be distinguished in confocal microscopy. But it still causes defective apical constriction, suggesting that a subtle difference in levels of these proteins can disorganize apical constriction. Our data show dispersed Rok and less prominent apicomedial myosin formation in *crb*, *E-Cad* and *baz* RNAi SGs, suggesting that changes in apical and junctional protein levels may affect the apical cytoskeletal networks to lead to apical constriction defects (Fig. 7).

Fog signaling activity is regulated by the MT networks

Fog signaling-dependent accumulation of Rok and myosin activation in the apicomedial region of the SG cells is critical for coordinated apical constriction during SG invagination (Chung et al., 2017). Here we show that Fog signaling activity is dependent on MTs. Overactivated Fog signaling by overexpression Fog is suppressed by loss of MTs (Fig. 5). Both the convoluted junctional phenotype in Fog-overexpressing cells and over-accumulated Rok in the apicomedial region are suppressed. Unlike other apical or junctional proteins that we have tested (Crb, E-Cad and Baz) that colocalize with Rab11/Nuf when mislocalized, mislocalized Fog did not co-localize with Rab11 or Nuf (data not shown). This can be explained by that Rab11 is primarily associated with recycling endosomes, and the ligand is ultimately degraded in most cases rather than recycled. Further work needs to be done to fully understand the mechanisms underlying trafficking of Fog and its receptor(s) to fully understand the regulatory mechanisms of the signaling pathway that generate cellular forces to drive cell shape changes during tissue morphogenesis.

Materials and Methods

Fly stocks and husbandry

Fly lines used in our experiments were listed in a separate table. All crosses were performed at 25°C, unless stated otherwise.

Antibody staining and confocal microscopy

Antibodies used in our experiments were listed in a separate table. Embryos were collected on grape juice-agar plates and processed for immunofluorescence using standard procedures. Briefly, embryos were dechorionated in 50% bleach, fixed in 1:1 heptane:formaldehyde for 40 min and devitellinized with 80% EtOH, then stained with primary and secondary antibodies in PBSTB (1X PBS, 0.1% Triton X-100, 0.2% BSA). For acetylated α-tubulin staining, embryos were hand-devitellinized. All images were taken with a Leica SP8 confocal microscope.

Cell segmentation and apical area quantification

Embryos immunostained with E-Cad and CrebA were imaged using a Leica SP8 confocal microscope. Maximum intensity projection was generated from three apical focal planes with highest E-Cad signals (0.3 um apart). Cells were segmented along the E-Cad signals and cell areas were calculated using the Imaris Program (Bitplane). All SGs used for quantification were invaginated within the range of 5.1- 9.9 um depth. Cell areas were color-coded within the range of 0 to 25 um2. Since the Imaris Program calculated the areas of both the front and the back of the projected cell layer, we divided the measured areas by two to get the true values of apical areas of SG cells. Therefore, the apical areas are about half the area that we previously reported in Chung et al., 2017.

Quantification of myosin intensity

Using the Imaris Program (Bitplane), we segmented individual SG cells based on E-Cad signals. Intensity mean of myosin of each segmented cell was measured. Correlation (Pearson) and Student t-test (Mann-Whitney) were calculated using the GraphPad Prism software.

Negative correlation between apical area and Rab11/Nuf intensity

Cell segmentation for five WT SGs at deep invagination was performed as described above. Intensity mean was measured for the entire Rab11/Nuf signals for each segmented cell and plotted. Correlation (Pearson) and P values were calculated using the GraphPad Prism software.

3D reconstruction of SGs

3D rendering of SGs was performed using the confocal stacks using the Imaris program.

Fly strains	**Source or reference**
UAS-Spastin (on II)	Sherwood lab (Duke; Sherwood et al., 2004)
UAS-Spastin-CFP (on III)	Sherwood lab (Duke; Du et al., 2010)
fkh-Gal4 (on II)	Andrew lab (John Hopkins; Chung et al., 2017)
fkh-Gal4 (on III)	Andrew lab (John Hopkins; Chung et al., 2017)
ubi-Rok-GFP	Abreu-Blanco et al., 2014
sqh-GFP	Royou et al., 2004
UAS-Rab11S25N-EYFP	Bloomington Stock Center (#9792, #23261)
UAS-Dicer-2	Bloomington Stock Center (#60008)
Dhc RNAi	Bloomington Stock Center (#76941, #28749) Vienna Drosophila Resource Center (v28053, v28054) 4 lines worked equally. v28054 was used for all of the data shown in this work.
$klar^{1}$	Bloomington Stock Center (#3256)
$klar^{mCD4}$	Bloomington Stock Center (#25097)
$klar^{mCD4}$ *ubi-Rok-GFP*	Recombinant line generated from $klar^{mCD4}$ and *ubi-Rok-GFP.*
Crb RNAi	Bloomington Stock Center (#38373, #38903, #40869, #34999) 4 lines worked equally. 2 lines (#38373, #34999) were used for the data shown in this work.

Baz RNAi	Bloomington Stock Center (#35002, #38213, #39072). #38213 showed strong invagination defects and was used for the data shown in this work.
ECad RNAi	Bloomington Stock Center (#32904)
UAS-Shg-GFP	Bloomington Stock Center (#58445)
UAS-Baz-GFP	Bloomington Stock Center (#65845)
matα-Gal4 (maternal Gal4; on II)	Bloomington Stock Center (#7062)

Antibody	**Source (catalog number)**	**Dilution**
α-E-Cad (rat)	DSHB (DCAD2)	1:50
α-CrebA (rat)	Andrew lab (John Hopkins)	1:3000
α-CrebA (rabbit)	Andrew lab (John Hopkins)	1:5000
α-Dhc (mouse)	DSHB (2C11-2)	1:50
α-Rab11 (rabbit)	Andrew lab (John Hopkins)	1:500
α-Nuf (guinea pig)	Sotillos lab (CABD)	1:500
α-acetylated α-tubulin (mouse)	Invitrogen (322700)	1:1000
α-GFP (chick)	Invitrogen (A10262)	1:500
α-β-galactosidase (rabbit)	Invitrogen (A11132)	1:500
α-Crb (mouse)	DSHL (Cq4)	1:10
α-Baz (guinea pig)	Zallen lab (Sloan Kettering Institute; Blankenship et al., 2006)	1:500
α-Baz (rabbit)	Zallen lab (Sloan Kettering Institute)	1:500
α-Fog (rabbit)	Fuse et al., 2013	1:1000
Alexa Fluor 488/568/647-coupled secondary antibodies	Invitrogen	1:500

Figure legends

Fig. 1. Intracellular trafficking components are apically enriched near the invagination pit. (A) A schematic drawing of the anterior region of the *Drosophila* embryo for stage 11 (ventral and lateral views) and stage 16 (lateral view). Top left, SG placodes are labeled in green. Top right, magnified view of a SG placode. Purple area, the region where SG cells undergo clustered apical constriction during invagination. (B-D) A wild type SG immunostained with E-Cad, Rab11 and Nuf. Rab11 and Nuf show upregulation in the apical region near the invagination pit. (B'-D') Heat maps of apical area (B') and intensity of Rab11 and Nuf (C', D'). Cells with small apical area (dark blue cells in B') near the invagination pit show high intensity of Rab11 and Nuf (red cells in C' and D'). (E) Negative correlation between Rab11/Nuf intensities and apical areas of SG cells. n=5 SGs (690 cells). $P<0.0001$. (F, G) Dhc64C is enriched near the invagination pit. (F', G') Heat maps corresponding to the SG placode shown in F and G. Asterisks: invagination pit.

Figure 1

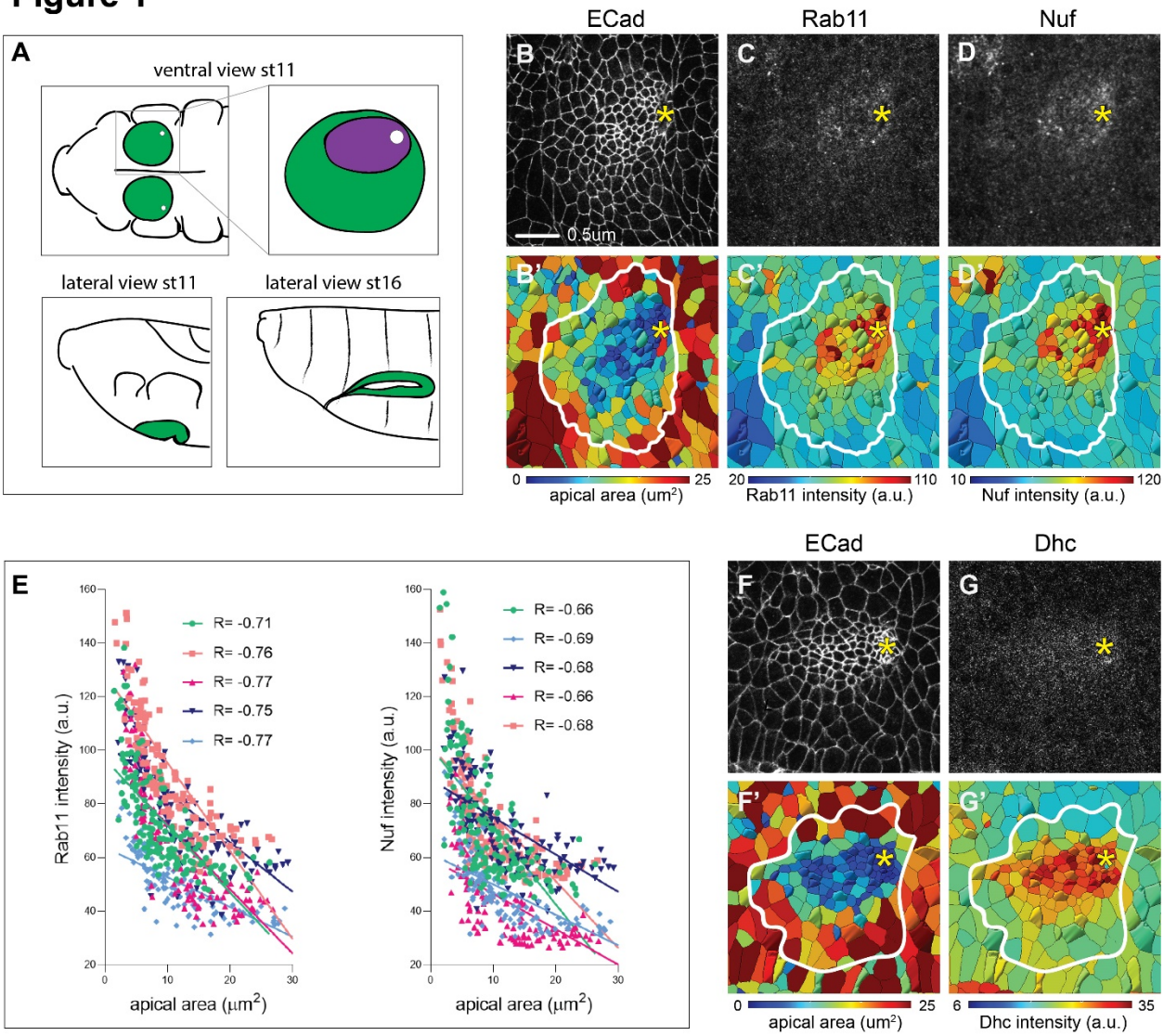

Fig. 2. Disruption of MTs results in uncoordinated apical constriction, reduction of apical vesicle numbers, and mislocalization of Rab11/Nuf.

(A-A’’’) Co-localization of Rab11 and acetylated α-tubulin in SG cells during invagination. A wild type SG immunostained with Rab11 (magenta) and acetylated alpha-tubulin (green) is shown with higher magnification of the yellow boxed area in A’-A’’’. Red arrowheads, co-localized Rab11 and acetylated α-tubulin. (B-C’) Overexpression of Spastin in the SG disrupts the MT networks. (B, B’) A control SG shows abundant levels of stable MTs labeled with acetylated α-tubulin. (C, C’) Overexpression of Spastin leads to loss of MTs in the SG. (D-F) Confocal images of a SG overexpressing Spastin stained with Rab11 and Nuf. (D’-F’) Color-coded images corresponding to D-F show defective apical constriction (D’) and significant reduction of Rab11 (E’) and Nuf (F’). (G) A ratio of deviation of Rab11 and Nuf intensity to median intensity in all SG cells. n= 5 SGs (690 cells), P values are calculated using the Mann-Whitney test, $p<0.0001$. (H-I’’’) Spastin overexpression causes mislocalization of Rab11 and Nuf in SG cells at stage 16. Higher magnifications of the yellow boxed area in H and I are shown in H’-H’’’ and I’-I’’’, respectively. (H-H’’’) In control, Rab11 and Nuf are enriched in the apical region of the SG cells (red arrows). (I-I’’’) Rab11 (I’’) and Nuf (I’’’) are mislocalized to big punctate structures in the cytoplasm in Spastin-overexpressing SGs. White dashed line, cell boundaries and nuclear membrane (H) and apical membrane (I). Asterisks: invagination pit. Nu, nucleus.

Figure 2

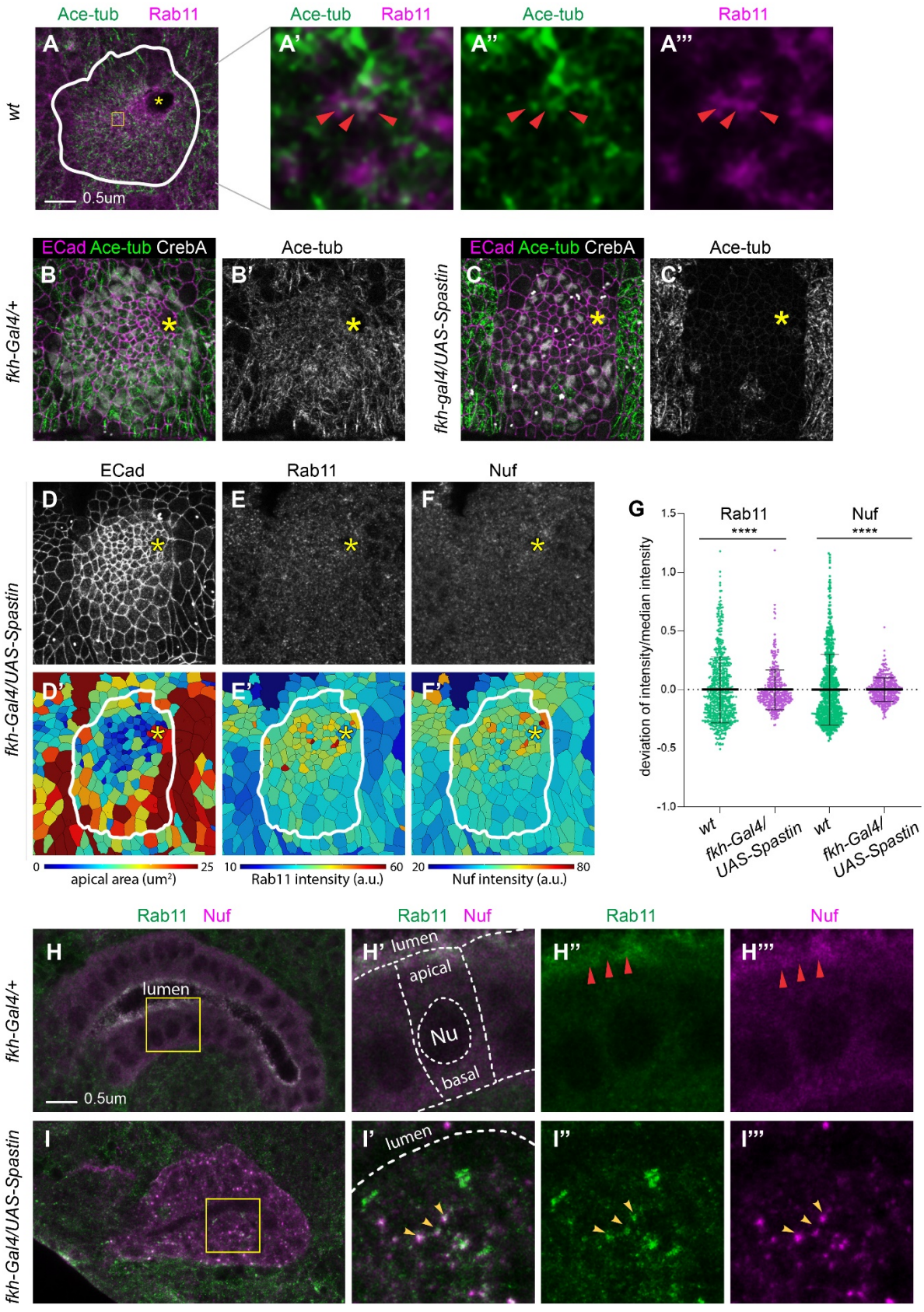

Fig. 3. Rab11 and the dynein motor are required for coordinated apical constriction in the SG.

(A-D') Confocal images of SGs of control (A), Rab11-DN-overexpression (B), *Dhc64C* RNAi (C) and *klar* mutant (D), stained with E-Cad.. (A'-D') Heat maps corresponding to images shown in A-D. SGs with disrupted intracellular trafficking show fewer cells with small apical area (dark blue cells) than control. (D, E) Percentage (D) and cumulative percentage (E) of cells with different apical area. P values are calculated using the Mann-Whitney U test (D) and the Kolmogorov-Smirnov test (E).****, $p<0.0001$. (F) 3D rendering of SGs stained with E-Cad (green) and CrebA (magenta). A range of phenotypes is observed when *Dhc64C* is knocked down both maternally and zygotically, including an enlarged pit, deformed epithelial tissue and additional folds. Asterisks: invagination pit.

Figure 3

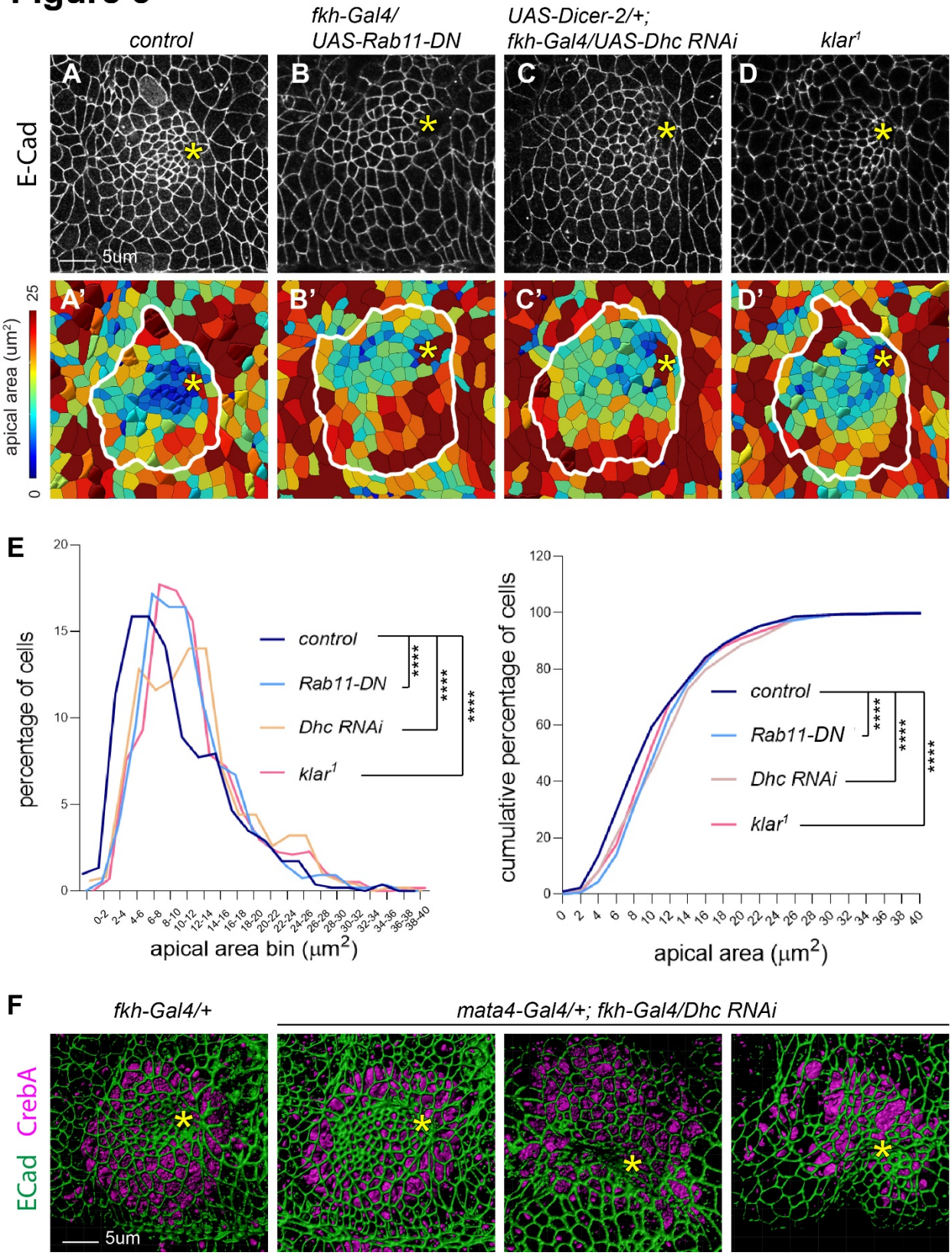

Fig. 4. Compromised intracellular trafficking leads to failure in accumulation of apicomedial Rok and reduction of apicomedial myosin formation in the SG cells

(A-D'') Control SG (A-A'') shows accumulation of Rok-GFP signals (green) in the apicomedial region of the cells near the invagination pit. E-Cad (magenta), cell boundary. (A'-D') Rok-GFP signals only. (A''-D'') Higher magnification of the yellow boxed area shown in A-D. (B-D'') Rok-GFP signals are more dispersed in SGs with Spastin overexpression (B-B'''), knockdown of *Dhc64C* (C-C'') and a mutation in *klar* (D-D''). In *Dhc64C* RNAi and *klar* mutant SGs, some big punctate structures of Rok-GFP were still observed occasionally. (E-G'') Myosin (sqh-GFP, green) signals in control (E-E''), *Dhc64C* RNAi (F-F'') and *klar* mutant (G-G'') SG. Magenta, E-Cad. (E'-G') sqh-GFP only. (E''-G'') Higher magnification of the yellow boxed area in E-G. *Dhc64C* RNAi and *klar* mutated SGs show reduced levels of apicomedial myosin, especially in the cells with bigger apical area. (H) Negative correlation between myosin intensity and apical area of the cells are calculated. Cells from five SGs of each genotype that are shown in E-G are plotted with different colors. Trendlines are shown for each SG. R, Pearson correlation coefficient. P values are calculated using Mann-Whitney test. ****, $p<0.0001$. Quantification for each genotype: *sqhGFP/+; fkh-Gal4/+*: n= 5SGs, 573 cells; *sqhGFP/UAS-Dicer-2; fkh-Gal4/UAS-Dhc RNAi*: n= 5SGs, 567 cells; *sqhGFP; klar1*: n= 5SGs, 572 cells; *klar1*: n= 6SGs, 704 cells. Asterisks: invagination pit.

Figure 4

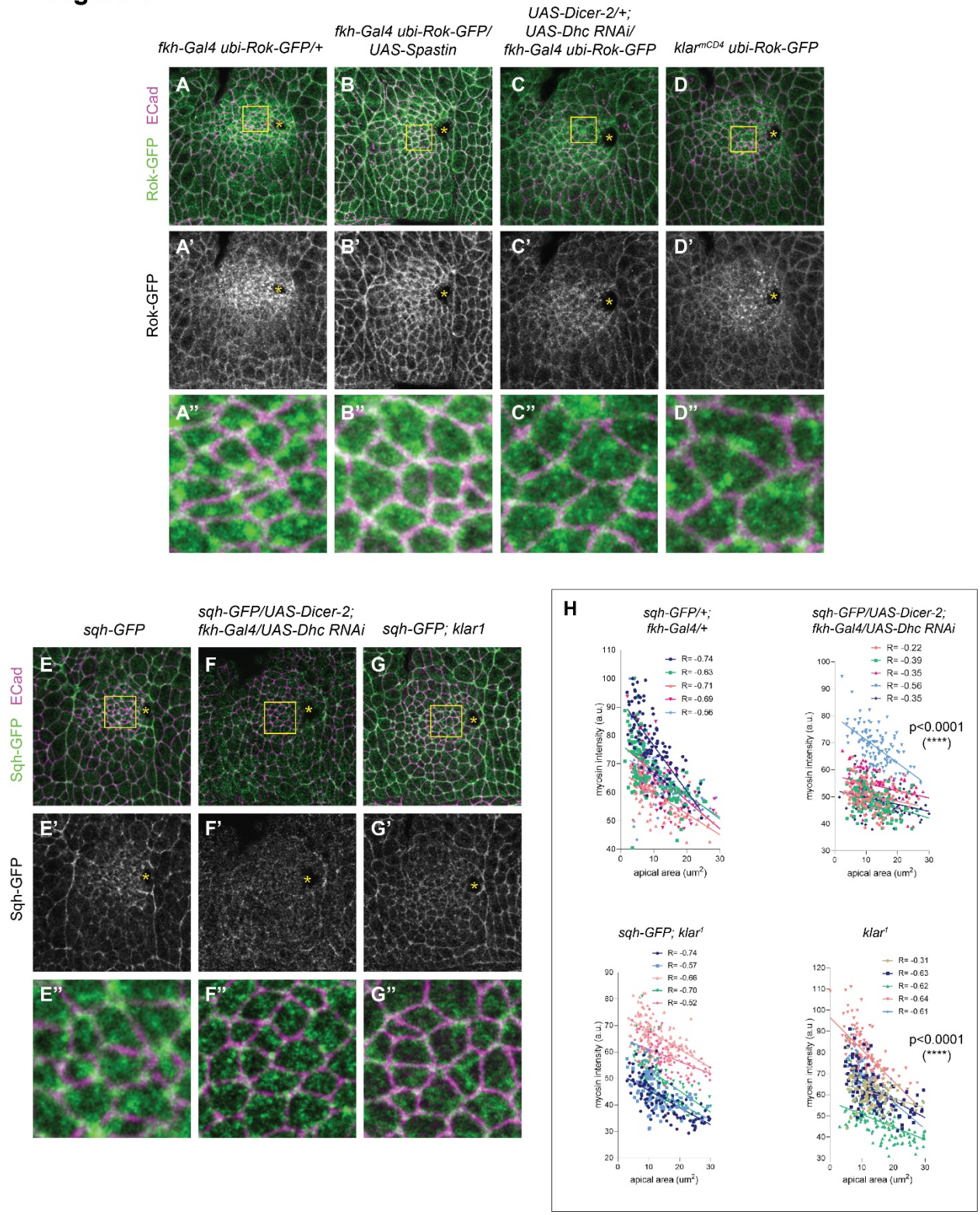

Fig. 5. Fog signaling activity is reduced when intracellular trafficking is compromised

(A-A’’’) SG expressed Rok-GFP is labeled with GFP (green), E-Cad (magenta). Rok-GFP signals are accumulated in the apical medial region as big punctate structures. (B-B’’’) SG is overexpressed Fog protein under the activation of fkh-Gal driver. Rok-GFP is over-accumulated in the cells near the invagination pit (B’). E-Cad signals show wiggly cell junctions (B’’). (C-C’’’) Overexpression of Spastin suppresses over-accumulation of Rok-GFP and the wiggly junctional phenotype caused by Fog overexpression. (A’’’-C’’’) Higher magnification of the yellow boxed area shown in A-C. Asterisks: invagination pit.

Figure 5

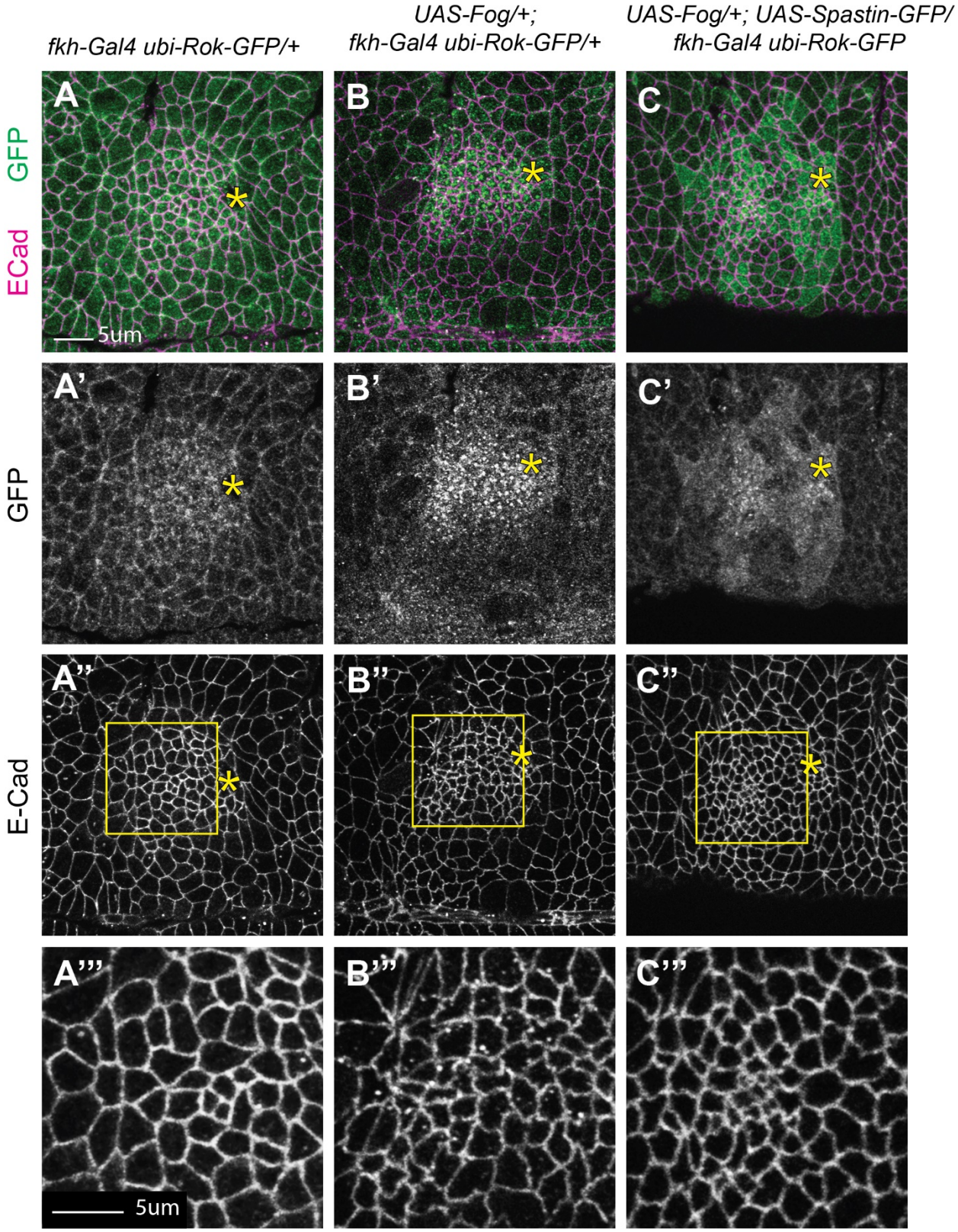

Fig. 6. MT-dependent intracellular trafficking regulates localization of Crb.

(A-C') Stage 11 SGs stained with Crb. Higher magnification of the yellow boxed area are shown in A'-C'. Compared to wild type control (A, A') Crb-overexpressing SGs show increase apical area (B, B'). (C-C') Co-overexpression of Spastin suppresses the enlarged apical area phenotype of Crb-overexpressing SG cells. (D-D''') In the basal region of the SG cells that co-overexpress Crb and Spastin, Rab11 (magenta) and Crb (green) are mislocalized as punctate structures. Yellow arrowheads show co-localization of Crb and Rab11. (E-F''') Stage 16 SGs that overexpress Crb (E'-E''') and co-overexpress Crb and Spastin (F-F'''). (E-E''') Overexpression of Crb results in overaccumulation of Crb in the apical region of the gland. Crb also localizes to the basolateral side of the cells. Rab11 localizes in the apical region as in wild type (see Fig. 2H-H''). (F-F''') Co-overexpression of Spastin and Crb leads to mislocalization of Crb in the cytoplasmic and basolateral region, consistent with the results of stage 11. Mislocalized Crb co-localizes with Rab11 (yellow arrowheads). (G-H''') Disruption of MTs results in aggregation of E-Cad to the basolateral region of SG cells. (G-G''') Overexpressed GFP-tagged E-Cad signals overlap with signals recognized by an E-Cad antibody. The majority of E-Cad-GFP maintains in the apical region and a minor level is localized in the basolateral region. (H-H''') Co-overexpression of Spastin and E-Cad-GFP in the SG results in mislocalized E-Cad-GFP to the basolateral region as big punctate structures (H'-H''', red arrowheads). (I-J''') Loss of MTs suppresses the enlarged lumen phenotype in the Baz-GFP-overexpressing SG and reduces the Baz-GFP levels in the apical region. (I-I''') Overexpression of Baz-GFP causes bigger lumen in the stage 16 SG. High levels of Baz-GFP are observed at adherens junctions, and a low level of Baz-GFP was detected in the basolateral region of SG cells. Nuf is enriched in the apical region of the SG cells. (J-J''') Co-overexpression of Baz-GFP and Spastin decreases junctional Baz-GFP signals and suppression of the enlarged lumen phenotype. Spastin overexpression leads to mislocalization of Nuf-positive vesicles to the basolateral and cytoplasmic region of the cells (blue arrows). Asterisks: invagination pit.

Figure 6

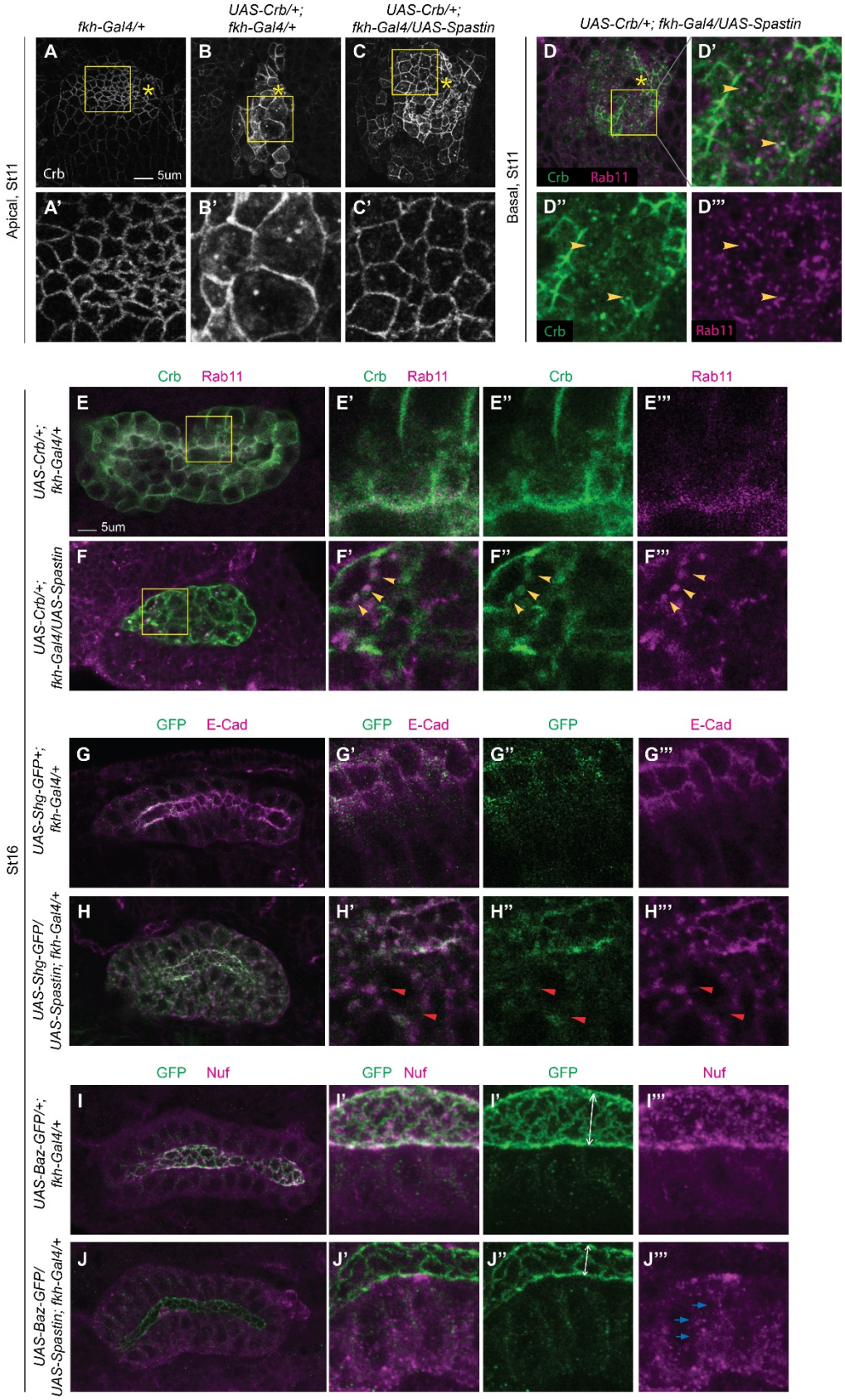

Fig. 7. Crb, E-Cad and Baz have a role in regulating apical constriction during SG invagination.

(A-D') Knockdown of *crb*, *E-Cad*, or *baz* results in apical constriction defects. (A-D) confocal images of SGs stained with E-Cad. (A'-D') Heat maps corresponding to images shown in A-D. Compared to control (A, A'), SGs with knockdown of *crb* (B, B'), *E-Cad* (C, C') and *baz* (D, D') show reduced number of cells that have small apical area (dark blue cells in heat maps). (E) (D, E) Percentage (D) and cumulative percentage (E) of cells with different apical area. P values are calculated using the Mann-Whitney U test (D) and the Kolmogorov-Smirnov test (E).*, $p<0.05$. ****, $p<0.0001$. Note that cumulative percentage of cells in *E-Cad* RNAi SGs show a similar trend to other genotypes, but statistically less significantly. (F-G') Knockdown of *E-Cad* in SGs leads to the discontinuous E-Cad signals at adherens junctions (red arrowheads) and significant reduced and discontinuous E-Cad signals along the basolateral membrane (yellow arrowheads) at stage 16. (F', G') Higher magnification of yellow boxed areas in H, I. Asterisks: invagination pit.

Figure 7

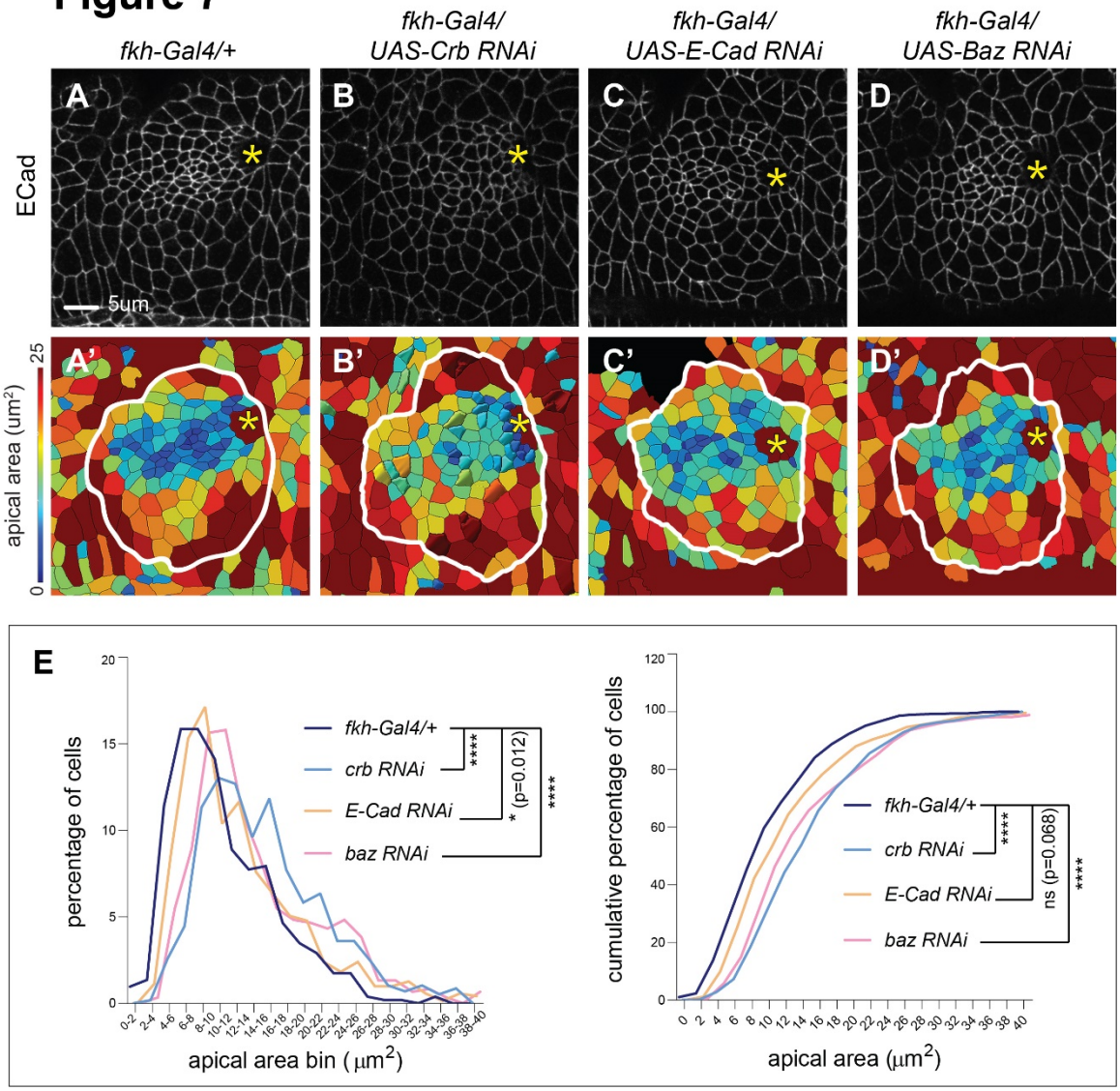

Fig. 8. Knockdown of *crb*, *E-Cad* or *baz* results in dispersed medial Rok and reduced apicomedial myosin formation. (A-D'') Knockdown of *crb*, *E-Cad* or *baz* leads to failure in accumulation of apicomedial Rok in SG cells near the invagination pit. (A"-D") Magnification of yellow boxes shown in A-D. (E-H") Knockdown of *crb*, *E-Cad* or *baz* results in reduction of apicomedial myosin in SG cells near the invagination pit. (E"-H") Higher magnification of yellow boxed areas shown in E-H. (I) Negative correlation between medial myosin intensity and apical area of the cells. Cells from five SGs of each genotype shown in E-H are plotted with different colors. Trendlines are shown for each SG. R, Pearson correlation coefficient. For quantification for each genotype: *sqh-GFP/+; fkh-Gal4/+*: n= 5 SGs, 573 cells (same control SGs used in Fig. 4H); *sqh-GFP/+; fkh-Gal4/UAS-Crb* RNAi: n= 5 SGs, 471 cells; *sqh-GFP/+; fkh-Gal4/UAS-E-Cad* RNAi: n= 5 SGs, 515 cells; *sqh-GFP/+; fkh-Gal4/UAS-Baz* RNAi: n= 5 SGs, 600 cells. Asterisks: invagination pit.

Figure 8

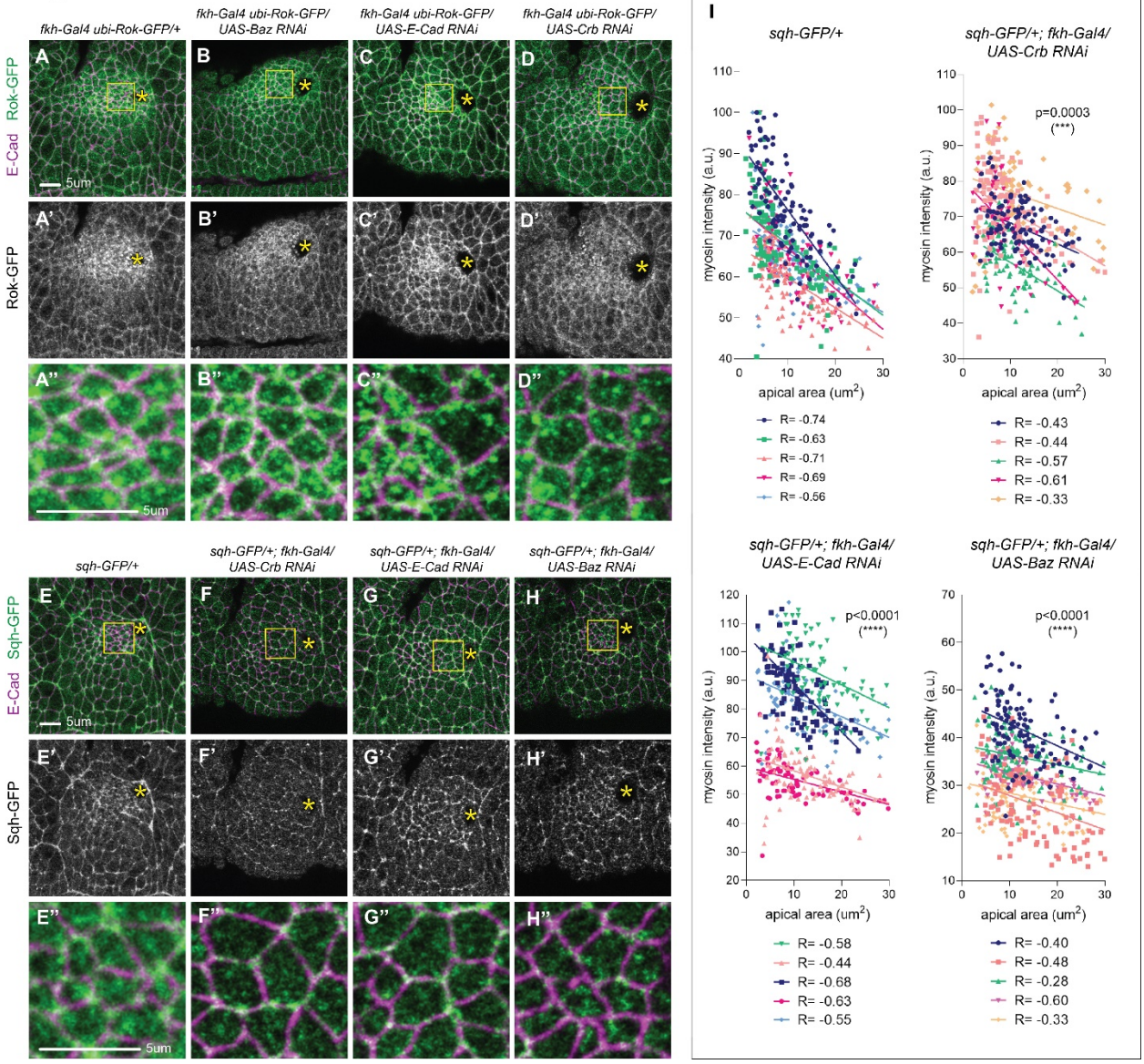

Supplemental Fig. 1. Rab5-EYFP, but not Rab7-EYFP, is enriched near the invagination pit during SG invagination. (A-B') *Rab5-EYFP* has an EYFP insertion into the endogenous Rab5 locus. (A, B) Confocal images of a Rab5-EYFP SG stained with E-Cad (A) and GFP (B). Rab5-EYFP signals are upregulated in the apical region near the invagination pit. (A', B') Heat maps of apical area (A') and intensity of Rab5-EYFP (B'). Cells with small apical area (dark blue cells in A') near the invagination pit show high intensity of Rab5-EYFP (red cells in B'). (C) Negative correlation between Rab5-EYFP intensity and apical areas of SG cells. n= 4 SGs (396 cells). (D-E') *Rab7-EYFP* has an EYFP insertion into the endogenous Rab7 locus. (D, E) A *Rab7-EYFP* SG immunostained with E-Cad (D) and GFP (E). (D', E') Heat maps of apical area (D') and intensity of Rab7-EYFP (E'). Rab7-EYFP signals are not upregulated in the apical region near the invagination pit. Asterisks: invagination pit.

Supplemental Fig. 1

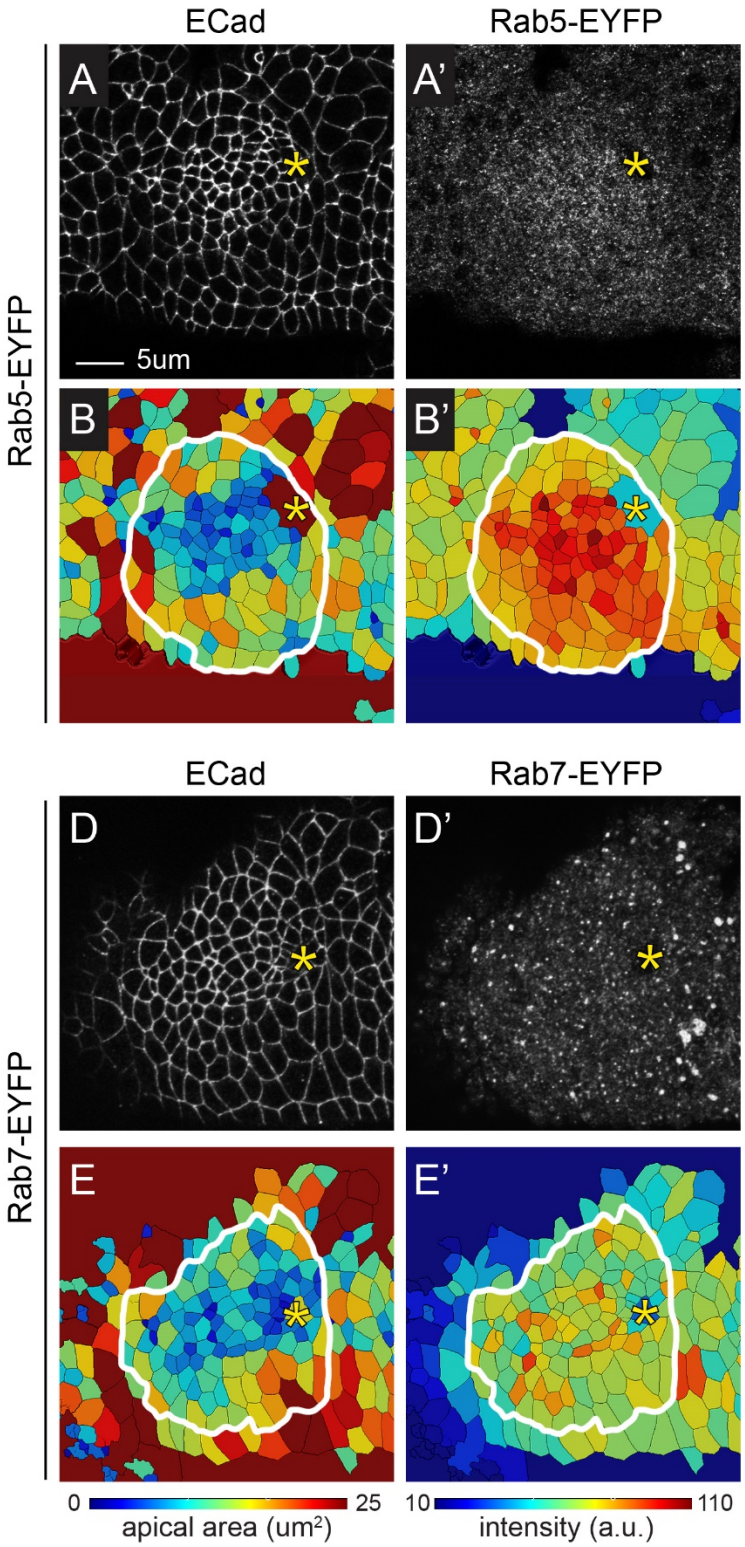

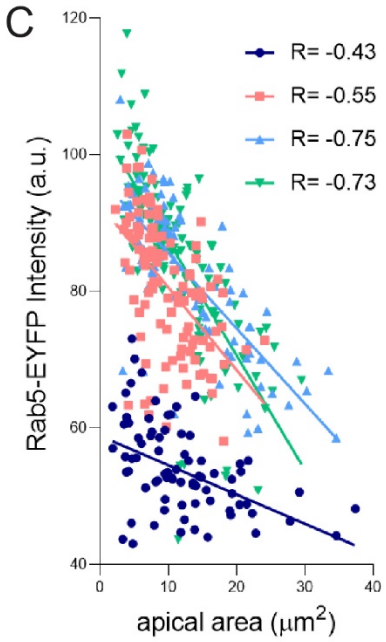

References

Abreu-Blanco, M. T., J. M. Verboon and S. M. Parkhurst (2014). "Coordination of Rho family GTPase activities to orchestrate cytoskeleton responses during cell wound repair." Curr Biol **24**(2): 144-155.

Aguilar-Aragon, M., G. Fletcher and B. J. Thompson (2019). "Apical transport of Crumbs maintains epithelial cell polarity." Biorxiv.

Andrew, D. J. and A. J. Ewald (2010). "Morphogenesis of epithelial tubes: Insights into tube formation, elongation, and elaboration." Dev Biol **341**(1): 34-55.

Booth, A. J. R., G. B. Blanchard, R. J. Adams and K. Roper (2014). "A dynamic microtubule cytoskeleton directs medial actomyosin function during tube formation." Dev Cell **29**(5): 562-576.

Chua, J., R. Rikhy and J. Lippincott-Schwartz (2009). "Dynamin 2 orchestrates the global actomyosin cytoskeleton for epithelial maintenance and apical constriction." Proc Natl Acad Sci U S A **106**(49): 20770-20775.

Chung, S. and D. J. Andrew (2014). "Cadherin 99C regulates apical expansion and cell rearrangement during epithelial tube elongation." Development **141**(9): 1950-1960.

Chung, S., C. D. Hanlon and D. J. Andrew (2014). "Building and specializing epithelial tubular organs: the Drosophila salivary gland as a model system for revealing how epithelial organs are specified, form and specialize." Wiley Interdiscip Rev Dev Biol **3**(4): 281-300.

Chung, S., S. Kim and D. J. Andrew (2017). "Uncoupling apical constriction from tissue invagination." Elife **6**.

Dawes-Hoang, R. E., K. M. Parmar, A. E. Christiansen, C. B. Phelps, A. H. Brand and E. F. Wieschaus (2005). "folded gastrulation, cell shape change and the control of myosin localization." Development **132**(18): 4165-4178.

Gross, S. P., M. A. Welte, S. M. Block and E. F. Wieschaus (2000). "Dynein-mediated cargo transport in vivo. A switch controls travel distance." J Cell Biol **148**(5): 945-956.

Guglielmi, G., J. D. Barry, W. Huber and S. De Renzis (2015). "An Optogenetic Method to Modulate Cell Contractility during Tissue Morphogenesis." Dev Cell **35**(5): 646-660.

Izquierdo, E., T. Quinkler and S. De Renzis (2018). "Guided morphogenesis through optogenetic activation of Rho signalling during early Drosophila embryogenesis." Nat Commun **9**(1): 2366.

Jouette, J., A. Guichet and S. B. Claret (2019). "Dynein-mediated transport and membrane trafficking control PAR3 polarised distribution." Elife **8**.

Kerridge, S., A. Munjal, J. M. Philippe, A. Jha, A. G. de las Bayonas, A. J. Saurin and T. Lecuit (2016). "Modular activation of Rho1 by GPCR signalling imparts polarized myosin II activation during morphogenesis." Nat Cell Biol **18**(3): 261-270.

Khanal, I., A. Elbediwy, C. Diaz de la Loza Mdel, G. C. Fletcher and B. J. Thompson (2016). "Shot and Patronin polarise microtubules to direct membrane traffic and biogenesis of microvilli in epithelia." J Cell Sci **129**(13): 2651-2659.

Ko, C. S., V. Tserunyan and A. C. Martin (2019). "Microtubules promote intercellular contractile force transmission during tissue folding." J Cell Biol **218**(8): 2726-2742.

Le Droguen, P. M., S. Claret, A. Guichet and V. Brodu (2015). "Microtubule-dependent apical restriction of recycling endosomes sustains adherens junctions during morphogenesis of the Drosophila tracheal system." Development **142**(2): 363-374.

Lee, J. Y. and R. M. Harland (2010). "Endocytosis is required for efficient apical constriction during Xenopus gastrulation." Curr Biol **20**(3): 253-258.

Letizia, A., S. Sotillos, S. Campuzano and M. Llimargas (2011). "Regulated Crb accumulation controls apical constriction and invagination in Drosophila tracheal cells." J Cell Sci **124**(Pt 2): 240-251.

Li, M., M. McGrail, M. Serr and T. S. Hays (1994). "Drosophila cytoplasmic dynein, a microtubule motor that is asymmetrically localized in the oocyte." J Cell Biol **126**(6): 1475-1494.

Manning, A. J., K. A. Peters, M. Peifer and S. L. Rogers (2013). "Regulation of epithelial morphogenesis by the G protein-coupled receptor mist and its ligand fog." Sci Signal **6**(301): ra98.

Martin, A. C. and B. Goldstein (2014). "Apical constriction: themes and variations on a cellular mechanism driving morphogenesis." Development **141**(10): 1987-1998.

Martin, A. C., M. Kaschube and E. F. Wieschaus (2009). "Pulsed contractions of an actin-myosin network drive apical constriction." Nature **457**(7228): 495-499.

Mason, F. M., M. Tworoger and A. C. Martin (2013). "Apical domain polarization localizes actin-myosin activity to drive ratchet-like apical constriction." Nat Cell Biol **15**(8): 926-936.

Miao, H., T. E. Vanderleest, C. E. Jewett, D. Loerke and J. T. Blankenship (2019). "Cell ratcheting through the Sbf RabGEF directs force balancing and stepped apical constriction." J Cell Biol.

Myat, M. M. and D. J. Andrew (2002). "Epithelial tube morphology is determined by the polarized growth and delivery of apical membrane." Cell **111**(6): 879-891.

Ossipova, O., K. Kim, B. B. Lake, K. Itoh, A. Ioannou and S. Y. Sokol (2014). "Role of Rab11 in planar cell polarity and apical constriction during vertebrate neural tube closure." Nat Commun **5**: 3734.

Rauzi, M., P. F. Lenne and T. Lecuit (2010). "Planar polarized actomyosin contractile flows control epithelial junction remodelling." Nature **468**(7327): 1110-1114.

Roeth, J. F., J. K. Sawyer, D. A. Wilner and M. Peifer (2009). "Rab11 helps maintain apical crumbs and adherens junctions in the Drosophila embryonic ectoderm." PLoS One **4**(10): e7634.

Roh-Johnson, M., G. Shemer, C. D. Higgins, J. H. McClellan, A. D. Werts, U. S. Tulu, L. Gao, E. Betzig, D. P. Kiehart and B. Goldstein (2012). "Triggering a cell shape change by exploiting preexisting actomyosin contractions." Science **335**(6073): 1232-1235.

Royou, A., C. Field, J. C. Sisson, W. Sullivan and R. Karess (2004). "Reassessing the role and dynamics of nonmuscle myosin II during furrow formation in early Drosophila embryos." Mol Biol Cell **15**(2): 838-850.

Sawyer, J. K., N. J. Harris, K. C. Slep, U. Gaul and M. Peifer (2009). "The Drosophila afadin homologue Canoe regulates linkage of the actin cytoskeleton to adherens junctions during apical constriction." J Cell Biol **186**(1): 57-73.

Sawyer, J. M., J. R. Harrell, G. Shemer, J. Sullivan-Brown, M. Roh-Johnson and B. Goldstein (2010). "Apical constriction: a cell shape change that can drive morphogenesis." Dev Biol **341**(1): 5-19.

Sherwood, N. T., Q. Sun, M. Xue, B. Zhang and K. Zinn (2004). "Drosophila spastin regulates synaptic microtubule networks and is required for normal motor function." PLoS Biol **2**(12): e429.

Wodarz, A., F. Grawe and E. Knust (1993). "CRUMBS is involved in the control of apical protein targeting during Drosophila epithelial development." Mech Dev **44**(2-3): 175-187.